A DNA functionalized advanced electrochemical biosensor for identification of the foodborne pathogen Salmonella enterica serovar Typhi in real samples

Bacchu, M. S., Ali, M. R., Das, S., Akter, S., Sakamoto, H., Suye, S-I., Rahman, M. M., Campbell, K., & Khan, M. Z. H. (2021). A DNA functionalized advanced electrochemical biosensor for identification of the foodborne pathogen Salmonella enterica serovar Typhi in real samples. *Analytica Chimica Acta*, Article 339332. Advance online publication. https://doi.org/10.1016/j.aca.2021.339332

Published in:
Analytica Chimica Acta

Document Version:
Peer reviewed version

Queen's University Belfast - Research Portal:
Link to publication record in Queen's University Belfast Research Portal

Journal Pre-proof

A DNA functionalized advanced electrochemical biosensor for identification of the foodborne pathogen *Salmonella enterica* serovar Typhi in real samples

M.S. Bacchu, M.R. Ali, S. Das, S. Akter, H. Sakamoto, S.-I. Suye, M.M. Rahman, K. Campbell, M.Z.H. Khan

PII: S0003-2670(21)01158-2

DOI: https://doi.org/10.1016/j.aca.2021.339332

Reference: ACA 339332

To appear in: *Analytica Chimica Acta*

Received Date: 10 October 2021

Revised Date: 21 November 2021

Accepted Date: 24 November 2021

Please cite this article as: M.S. Bacchu, M.R. Ali, S. Das, S. Akter, H. Sakamoto, S.-I. Suye, M.M. Rahman, K. Campbell, M.Z.H. Khan, A DNA functionalized advanced electrochemical biosensor for identification of the foodborne pathogen *Salmonella enterica* serovar Typhi in real samples, *Analytica Chimica Acta* (2021), doi: https://doi.org/10.1016/j.aca.2021.339332.

Author contributions:

M.Z.H. Khan planned the work and designed the experiment. M. R. Ali, M. S. Bacchu and S. Das carried out experimental work. S. Akter supervised microbiology part of this experiment. H. Sakamoto and S-I. Suye and K. Campbell performed calculated data and have written some part of the manuscript and revised the manuscript.

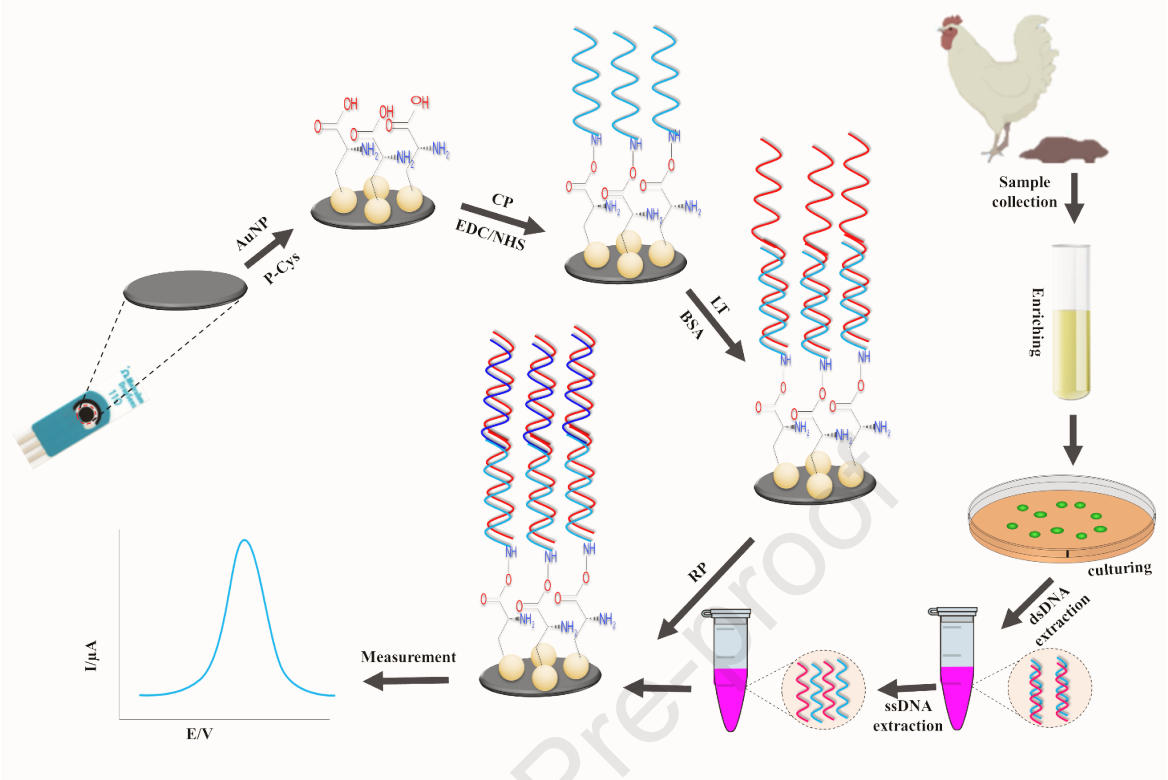

A DNA functionalized advanced electrochemical biosensor for identification of the foodborne pathogen *Salmonella enterica* serovar Typhi in real samples

M. S. Bacchu[1,2], M. R. Ali[1,2], S. Das[3], S. Akter[3], H. Sakamoto[4,5], S-I. Suye[4,5], M. M. Rahman[6], K. Campbell[7], M. Z. H. Khan[1,2*]

[1]*Dept. of Chemical Engineering, Jashore University of Science and technology, Jashore 7408, Bangladesh*

[2]*Laboratory of Nano-bio and Advanced Materials Engineering (NAME), Jashore University of Science and technology, Jashore 7408, Bangladesh*

[3]*Dept. of Microbiology, Jashore University of Science and technology, Jashore 7408, Bangladesh*

[4]*Department of Frontier Fiber Technology and Science, Graduate School of Engineering, University of Fukui, 3-9-1 Bunkyo, Fukui, 910-8507, Japan.*

[5]*Life Science Innovation Center, University of Fukui, Fukui, 910-8507, Japan*

[6]*Faculty of Science and Information Technology, Daffodil International University, Dhaka 1207, Bangladesh*

[7]*Institute for Global Food Security, School of Biological Sciences, Queen's University, 19 Chlorine Gardens, Belfast BT9 5DL, UK.*

*Corresponding author: zaved.khan@just.edu.bd

Abstract

An efficient platform for the detection of *Salmonella enterica* serovar Typhi (*S. Typhi*) is essential for early-stage diagnosis of typhoid to prevent and contain outbreaks. Here, we fabricated an electrochemical DNA biosensor for selective identification of *S. Typhi* in real samples. The biosensor has been fabricated by immobilizing an amine labelled *S. Typhi* specific single-strand capture probe on the surface of gold nanoparticles (AuNP) and poly cysteine (P-Cys) modified screen-printed electrode. Differential pulse voltammetry (DPV) of anthraquinone-2-sulfonic acid monohydrate sodium salt (AQMS) as a signal indicator was monitored to detect *S.* Typhi by hybridization of target DNA with the probe DNA. The fabricated biosensor shows a detection range of 1×10^{-6} to 1×10^{-22} molL^{-1} with a LOD of 6.8×10^{-25} molL^{-1} in *S.* Typhi complementary linear target and 1.8×10^{5} to 1.8 CFUml^{-1} with a LOD of 1 CFUml^{-1} in a real *S.* Typhi sample. The biosensor shows excellent discrimination ability to some bases mismatched and different bacterial cultures (same and distant genera). The most beneficial points of the proposed DNA biosensor are the lower limit of detection and the ability to reuse the biosensor more than 6 to 7 times. In addition, the practicability of the biosensor was investigated via detecting *S.* Typhi in blood, poultry feces, egg, and milk whereby excellent recoveries ranging from 96.54 to 103.47% were demonstrated indicating that this biosensor might be the most promising diagnostic tool for monitoring *S.* Typhi in clinical and food samples.

Keywords: Typhoid; Biosensor; *Salmonella* Typhi; poly cysteine; DNA sensor; electrochemical engineering.

1.0 Introduction

The global economy and human health are facing a noticeable threat due to foodborne diseases caused by pathogenic bacteria [1–4]. Among them, the most common foodborne pathogen is *Salmonella* which causes several symptoms and uncertain death. *Salmonella* is a gram-negative rod-shaped bacteria from the Enterobacteriaceae family [5,6]. The World Health Organization (WHO) certified that *Salmonella* is a member of four major global diarrheal pathogens which have some resistant serotypes (WHO-2018). *Salmonella bongori* (*S. bongori*) and *Salmonella enterica* (*S. enterica*) are the two main species having more than 2.5 thousand serotypes that all can cause severe infections (vomiting, dehydrating diarrhea, gastroenteritis, and typhoid) [7–9]. *Salmonella* bacteria are classified according to the Kauffman-White classification scheme. The identification of serotypes is based on either the "O" (somatic/cell wall) antigens which consist of the lipopolysaccharide-protein chains exposed on the cell surface and "H" (flagellar) antigens. The different antigens are numbered and each serotype is given an antigenic formula and classified into a group.

The foodborne pathogen *Salmonella enteric* serovar Typhi (*S.* Typhi) is responsible for the life-threatening illness typhoid [10] which has a high mortality and morbidity rate. For human infections, poultry and poultry products are the prevalent food contamination-related sources of *S.* Typhi [11]. Conventional testing methods (culture and Widal test) suffer a lot of limitations and cannot detect the bacterium at the early stages of infection which is the major cause for higher mortality and morbidity rates of typhoid disease. Currently, the gold standard for typhoid diagnosis is the blood culture method but it takes several days for identification and the antibody-antigen-based Widal test isn't reliable due to the interference of some other fever-type diseases like malaria, brucellosis, and hepatitis [12]. On the other hand, the advanced screening methods (PCR,

ELISA, southern hybridization, NGS) are highly expensive, sophisticated, and require experienced personnel [13,14]. The identification of *S. Typhi* at an early stage is still challenging. Hence, it is necessary to develop a new reliable detection method for the proper identification of *S.* Typhi for accurate diagnosis as well as monitoring the quality of food and the environment. Recently, molecular biotechnology and bioelectronics have enabled a promising technique (electrochemical DNA biosensor) for selective and sensitive detection of various microorganisms of interest [15–22]. Nucleic acid (DNA or RNA) hybridization-based electrochemical DNA biosensor provides benefits of specificity[23], sensitivity[24], miniaturization[25], reusability[26], cost effectivity[27] and compatibility to a micro-structure sensing assay compared to existing techniques [28]. In electrochemical DNA biosensor, free electron or charge produce due to the biological interaction of biorecognition element (such as ssDNA probe, Aptamer) and target (here *S.* Typhi) and causing the electric current, potential, or other electrical characteristics of the solution to change. A transducer can transform the biological signal into a detectable electrical signal proportional to the target concentration, which can then be displayed on a computer[29]. To enhance the electroanalytical performance of electrochemical DNA biosensors, various nanomaterials are used to immobilize bio-receptors on the surface of the electrode for detecting specific targets [30]. Among them, gold nanoparticles (AuNPs) are widely used in biosensing applications for enhancing the signal response, sensitivities, and immobilization activity of receptors on electrode surfaces [31,32]. L-Cysteine (L-Cys) is an amino acid applied for modification of the electrode surface. It contains a thiol group (-SH), amino group ($-NH_2$), and a carboxylic group (-COOH), in which the thiol group can strongly bond with metal (especially Au, Ag, Pt) and the carboxylic group can bind with amine labelled DNA probes [33–35].

In this study, we proposed an electrochemical DNA-based biosensor for the identification of *S.* Typhi in food and clinical samples by using DNA immobilized modified SPE. The electrode was modified by using AuNP and P-Cys via an electropolymerization technique and characterized by different voltammetric and morphological techniques. The sensor detects *S.* Typhi by using the increased oxidation current response of AQMS. The proposed biosensor shows some exceptional performance in terms of LOD, reusability, sensitivity, stability, and discrimination ability compared to previously reported work (refs required here).

2.0 Experimental section

2.1 Chemical and Reagents

L-Cysteine, Gold (III) chloride ($HAuCl_4$), trisodium citrate were purchased from Aladdin reagent Ltd. (China). The crosslinkers 1-Ethyl-3-(3-dimethyl aminopropyl)carbodiimide (EDC) and N-hydroxysuccinimide (NHS) were bought from Sigma Aldrich (China). The different agars and broth used for bacterial isolation and characterization (Muller Hinton agar, Mac Conkey agar, xylose lysine deoxycholate (XLD) agar, Simmons's Citrate Agar, Kligler Iron Agar, Selenite cystine broth) were purchased from OXOID (UK). QuickExtract™ DNA Extraction Solution used as the DNA extraction kit was purchased from Lucigen (USA). Phosphate buffer saline purchased from Sigma Aldrich (China) was chosen as a supporting electrolytic solution for all runs. Ultrapure water from Evoqua (Germany) of resistivity >18MΩcm^{-1} was used to make all solutions for this experiment. Other reagents used in this research were the highest analytical grade of purity. The oligonucleotide sequences (3' to 5') of the capture probe (StyR36-CP), linear target (StyR36-LT), reporter probe (StyR36-RP), bases mismatches, and non-complementary linear target (NCLT) as shown in **Table S1** were purchased from Sangon Biotech (China).

2.2 Instrumentation

Surface characterization of the different modified electrodes was investigated with ATR-FTIR spectroscopy using a NICOLET iS20 and by SEM using a ZEISS Gemini SEM 500. CV, DPV, and EIS were conducted by using a Metrohm DropSens μStat-i 400s. SPE (Metrohm, 110) of the three-electrode system was used for electrochemical measurements.

2.3 Synthesis of AuNPs

To synthesize AuNP, a simple sodium citrate method was followed which was reported previously [36]. In brief, 200μl of 3M $HAuCl_4$ was added to 212 ml ultrapure water and boiled under reflux conditions. When the solution reached boiling point, 12.5 ml of 10mg/ml trisodium citrate was added to the solution and the solution was stirred vigorously for 30 minutes. Finally, the resulting solution was cooled and filtered several times for removing impurities.

2.4 *Fabrication of SPE/P-Cys@AuNP*

Firstly, L-Cys of 1×10^{-3} $molL^{-1}$ was dispersed in a 10 ml PBS solution of pH 6.0 and stirred continuously for 30 min. After that, 25 μl of the previously synthesized AuNPs were added to the solution and a homogenous solution was prepared by continuously stirring for 10 min. The SPE was immersed into the resulting solution and electropolymerized through the CV of 10 cycles from a potential range of -0.8V to 2.0V at the rate of 100 mV/s[37]. After completing the electropolymerization step, the resulting P-Cys and AuNP modified SPE (SPE/P-Cys@AuNP) electrodes were rinsed with PBS and used for further modification.

2.4 Preparation of the biosensor

NHS of 5×10^{-3}molL^{-1} and EDC of 2×10^{-3}molL^{-1} were dispersed in water and stirred until a homogenous solution was obtained. The SPE/P-Cys@AuNP was immersed in the resulting solution for 1 hour to activate and stabilize the -COOH group of P-Cys. Here, the function of EDC is to activate the -COOH group as a coupling agent and convert it into an amine-reactive ester to bind the -NH_2 of the CP by using NHS [38]. Then, the crosslinked electrode was rinsed by using ultrapure water and immersed into 0.01molL^{-1} containing 5×10^{-6} molL^{-1} of CP to immobilize the amine active CP on the previously modified electrode. The non-immobilized CP was removed by washing with PBS after overnight immobilization at 4ºC. Bovine serum albumin (BSA) of 1% was used to block unspecific sites of SPE/P-Cys@AuNP/CP by immersing the electrode in the BSA for 1 hour. Then, the complementary linear targets (LT) were bound to the CP by dipping the resulting CP immobilized electrode into PBS consisting of 1×10^{-3}molL^{-1} AQMS is a hybridization redox indicator and different concentrations of complementary linear targets (LT) at 4ºC. After completing 1-hour hybridization periods, the modified electrode was rinsed with PBS and immersed into RP solution which contains 1×10^{-6} molL^{-1} RP and 1×10^{-3}molL^{-1} AQMS in 0.01 molL^{-1} PBS. Finally, the electrode was rinsed with PBS and stored at 4ºC for further application.

2.5 Extraction of ssDNA

One loop full of collected bacterial culture (the procedure mention in supplementary section 1) was suspended into 500 µl of nano-pure water. It was centrifuged at 12,000 × g for 10 minutes. The pellet was collected and 100 µl of both nuclease-free water and Lucigen DNA buffer were added to the collected pellet. After vortex mixing, the DNA solution was heated at 65°C for 15 minutes. The DNA concentration was measured using a nanodrop spectrophotometer at 260nm. A double-stranded DNA solution (5ng/mL) was taken and again heated at 100°C for 10 minutes. The

resulting solution was immediately transferred into ice and kept for 3 to 4 minutes. The prepared single-stranded DNA was hybridized at the electrode surface at 57°C for 1 hour in the presence of 0.1 molL^{-1} AQMS. The detailed workflow is described in **Fig. S1**.

2.6 Procedure to detect S. Typhi

The DPV technique was adopted to detect *S.* Typhi complementary target DNA sequences in the presence of $1 \times 10^{-3}\, molL^{-1}$ AQMS in PBS at a potential range of -1V to 0V. Other DPV conditions for detection of *S.* Typhi were pulse width 0.1s, pulse periods 0.5s, and amplitude 0.1V. The peak current was calculated by comparing the peak current of AQMS from that of AQMS in the presence of the *S.* Typhi target. A similar method was followed to calculate the limit of detection (LOD) as previously reported. The step-by-step modification process to detect *S.* Typhi is shown in scheme 1.

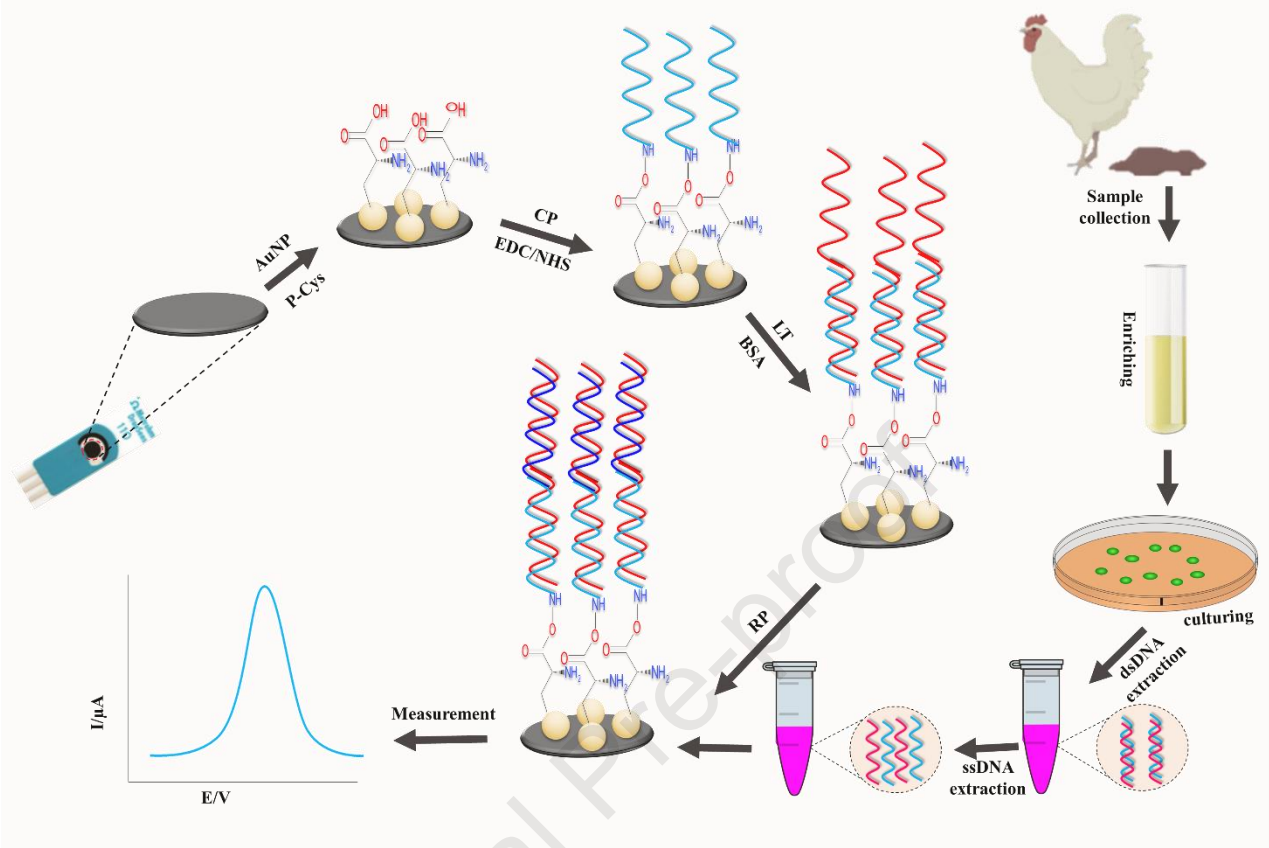

Scheme-1: Systematic procedure for the fabrication of the electrochemical DNA biosensor and detection of *S.* Typhi from real samples

2.7 Real sample preparation

To detect *S.* Typhi in the presence of spiked real samples of human blood, raw milk, egg, and poultry feces, DPV measurements of *S.* Typhi target DNA in these spiked samples were recorded. To prepare the fortified samples, *S.* Typhi of 2.1×10^5 $CFUml^{-1}$ was mixed with 100 mg of sample and 400 µl of normal saline. After vortexing, this prepared suspension of *S.* Typhi was added to 100 µl of each of the real samples. The single-stranded DNA was prepared according to the protocol described previously (Section 2.5). For the real sample's analysis, the isolation and primary identification of *S.* Typhi are provided in Supplementary Section 2.

3.0 Results and discussions

3.1 Preliminary study

3.1.1 Electropolymerization of P-Cys@AuNP on the surface of SPE

A CV method was adopted to electropolymerized P-Cys@AuNP on the surface of the SPE at a potential range of -0.8V to 2.0V. Figure 1A illustrates the cyclic voltammogram of P-Cys@Au on an electrode surface. Oxidation and reduction peaks were observed at the first cycle of deposition and the peak's current responses were enhanced as the number of cycles increased suggesting the nanocomposite had been attached to the surface of the SPE [39]. The attachment of P-Cys@AuNP was also validated by conducting an SEM image.

3.1.2 Surface characterization of SPE/P-Cys@AuNPs

To investigate the structural morphology of as-prepared AuNP and P-Cys@AuNP on the electrode surface, SEM and FTIR measurements were carried out. Figure 1B shows the FTIR spectrum of L-Cys, AuNPs, and P-Cys@AuNPs, wherein the amino acid L-Cys shows peaks at 3470cm^{-1}, 2550cm^{-1}, 1580cm^{-1}, 1070cm^{-1} for stretching O-H, S-H, C=O, and C-N respectively. As shown in P-Cys@AuNPs the weak stretching peak at 2550cm^{-1} of the thiol group disappears due to the formation of Au-S [40,41]. Figure 1C shows an SEM image of AuNP. The average diameter of AuNPs is approximately 35nm. Figure 1D shows the SEM image of GCE/P-Cys@AuNP which revealed the AuNP was decorated on the polymeric surface of P-Cys.

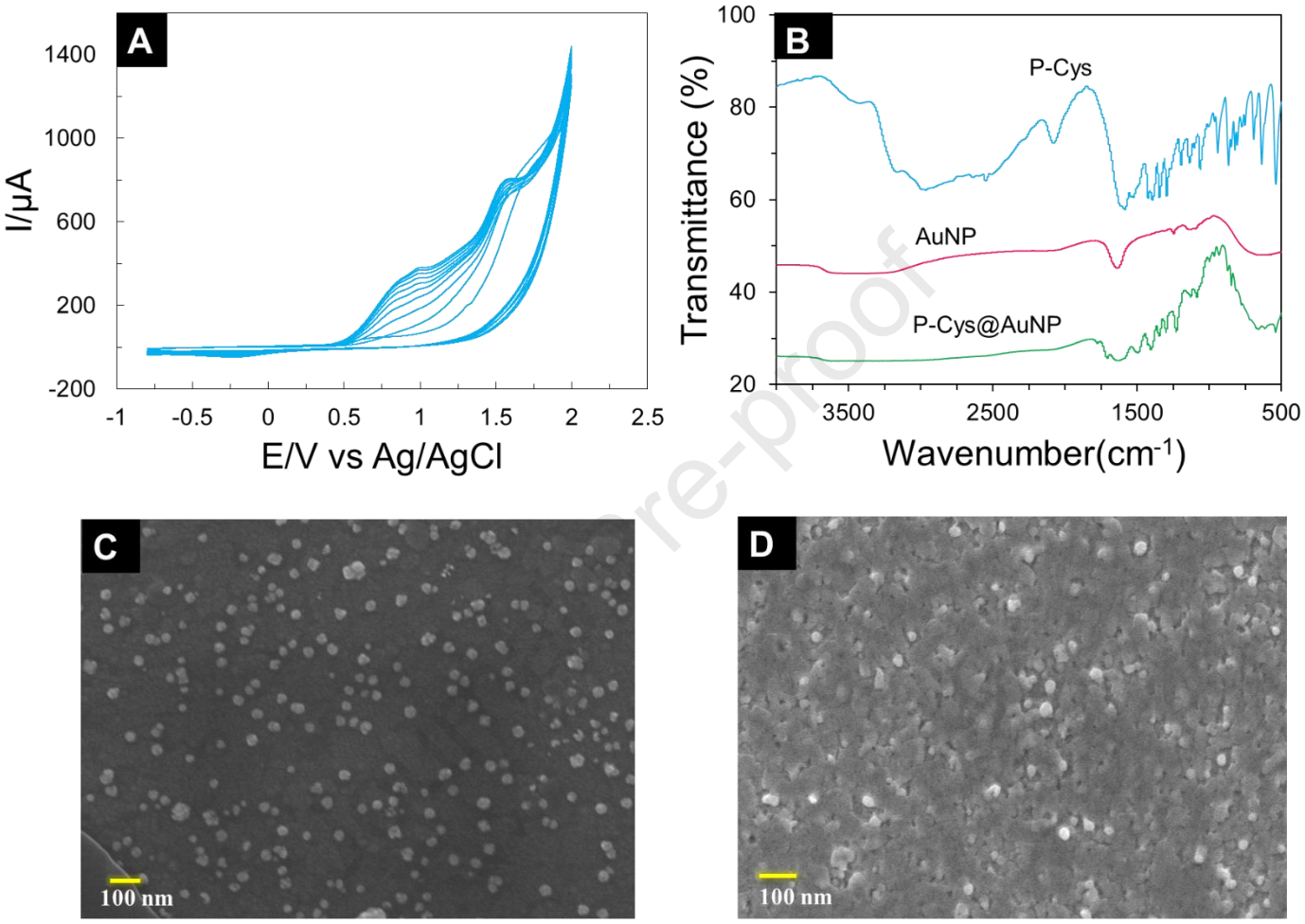

Figure 1: A series of 10 consecutive cycles of cyclic voltammogram recorded between -0.8V to 2.0V at a scan rate of 100mV/s in the solution containing L-Cys@AuNPs in PBS (A), ATR-FTIR spectroscopy of P-Cys, AuNP, and P-Cys@AuNP (B), SEM image of AuNP (C) and P-Cys@AuNP (D).

3.2 Feasibility study of electrochemical detection of S. Typhi

To develop an electrochemical biosensor, it is important to study the kinetics, surface chemistry, and optimized conditions of the electrode process. The well-known electrochemical methods CV

and the EIS are effectively used to investigate the sequential modification of the electrode surface for electrochemical measurement. In a CV method, typically, the signal pick of the CV increases with the higher rate of electron transfer and decreases with the lower conductance. The size of the semicircle of the EIS system indicates the charge transfer resistance (Rct) at the high-frequency region in terms of Faraday current. The larger the diameter of the semicircle demonstrated the higher Rct value and lower the electron transfer rate.

The feasibility of the designed electrochemical biosensor was investigated by using the CV method in 0.1 M KCl including 5.0×10^{-3} M $[Fe(CN)_6]^{3-/4-}$ solution for post-immobilization and hybridization processes (Fig. 2A). The biosensor showed an excellent electrocatalytic response within a neutral environment. AuNP modified SPE/P-Cys electrode (Fig. 2A(iii)) showed an excellent electron transfer process in comparison with the bare SPE (Fig. 2A(i)) and SPE/P-Cys electrode (Fig. 2A(ii)). These electrocatalytic phenomena demonstrated that the SPE/P-Cys@AuNP modified electrode obtained the maximum electrochemical active surface area and high electron transfer kinetics. The CP DNA was immobilized on the modified electrode surface through non-covalent binding between the rings of the nucleobases and the P-Cys@AuNP nanoplatforms. After immobilization of the CP a significant decrease in the self-redox signals was observed (Fig. 2A(iv)). The loaded CP acted as a random coil, which confirmed the immobilization on the sensor and prevented an effective electrode response [42]. The catalytic current decreased significantly after BSA was loaded (Fig. 2A(v)) and partial hybridization with LT (Fig. 2A(vi)) and then complete hybridization with RP (Fig. 2A(vii)).

Electrochemical impedance spectroscopy (EIS) experiments were also performed to confirm the feasibility of the fabricated biosensor with the synergy between different modified electrodes and the results were fitted in Fig. 2B. In 5.0×10^{-3} mM $[Fe(CN)_6]^{3-/4-}$ redox solution containing 0.1 M

KCl, the EIS response of the bare electrode showed a small semicircle (Fig. 2B(i)), an indication of good electron transfer rate. After loading the non-conductive P-Cys on the bare SPE surface (Fig. 2B(ii)), the Rct value increased in comparison with the bare electrode. The non-conductive P-Cys passivated the electrode surface and thus, blocked the electron transfer pathway. The value of Rct decreased after incorporation of the AuNP with P-Cys on the SPE (Fig. 2B(iii)). The highly conductive AuNP enhanced the electron transfer between the SPE surface and its corresponding modified layers and positively influenced the electrochemical charge transfer phenomena. When the CP was immobilized on the modified electrode surface (SPE/P-Cys@AuNP), a remarkable change of EIS response with a comparatively large semicircle (Fig. 2B(iv)) was observed of high Rct value of about 702Ω. Subsequently, the surface of the modified SPE/P-Cys@AuNP/CP electrode was covered more and hindered the electron transfer rate with a further increased noticeable value of Rct after BSA was loaded (Fig. 2B(v)) and the ssDNA of LT (Fig. 2B(vi)) and RP (Fig. 2B(vii)) were bound. When the amplified sequences are added to the electrode surface, these are fitted to the loop region of the molecular switch, which increased the phosphate skeleton on the electrode surface and decreased the electron transfer rate [43]. The EIS also confirmed that the Rct value after incubation in LT and RP is changed to 997Ω and 1090 Ω respectively, higher than that of incubation after CP.

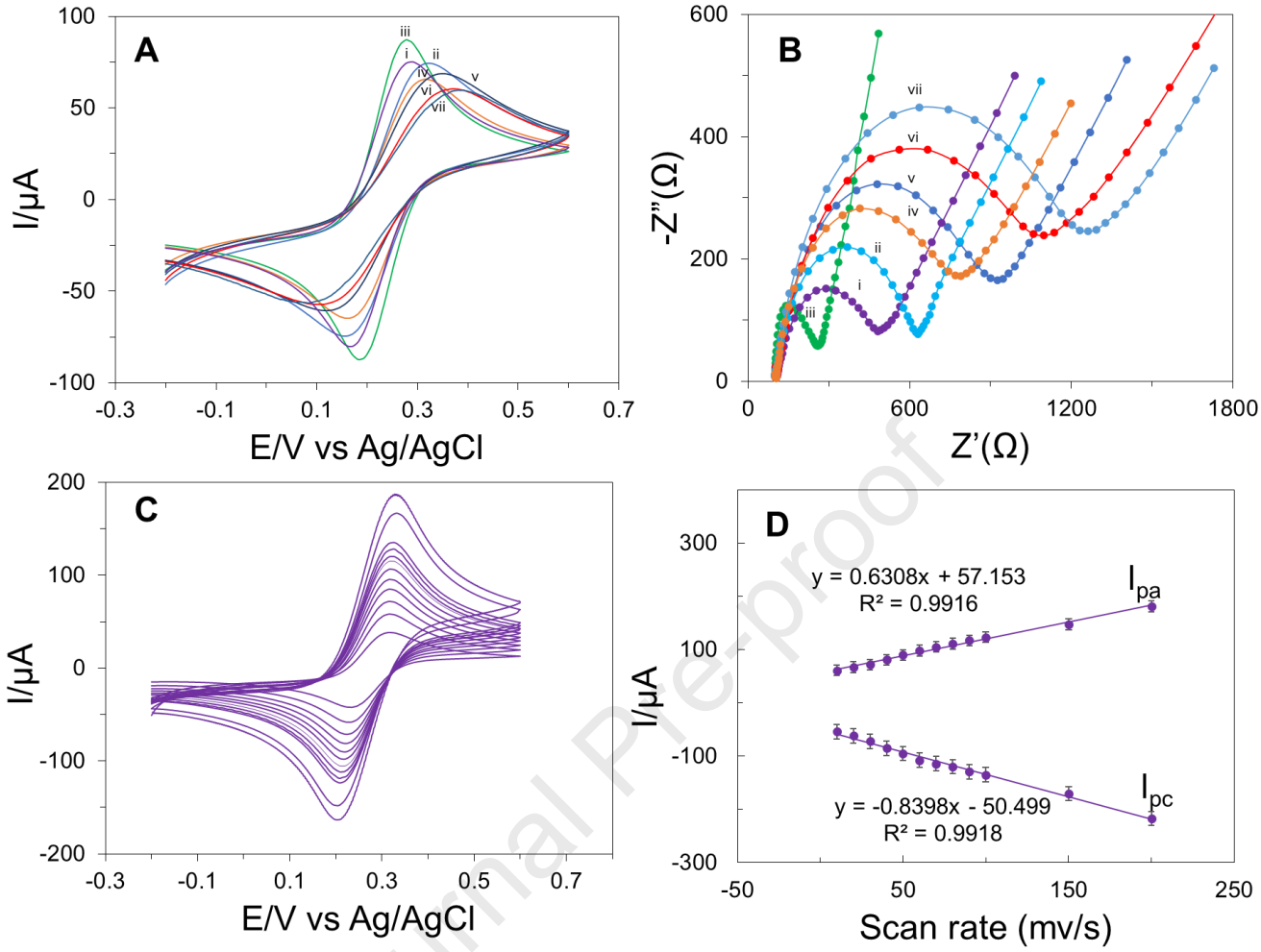

Figure 2: Cyclic voltammograms (A) and Nyquist plot of EIS (B) of the different electrodes measured in 0.1 M KCl including 5.0×10^{-3} M $[Fe(CN)_6]^{3-/4-}$: (i) bare SPE, (ii) SPE/P-Cys, (iii) SPE/P-Cys@AuNP, (iv) SPE/P-Cys@AuNP/CP, (v) SPE/P-Cys@AuNP/CP/BSA, (vi) SPE/P-Cys@AuNP/CP/BSA/LT and (vii) SPE/P-Cys@AuNP/CP/BSA/LT/RP.(C) CV response obtained for SPE/P-Cys@AuNP sensor different scan rates (from inner to outer): 10, 20, 30, 40, 50, 60, 70, 80, 90, 100, 150 and 200 mV/s in 0.1 M KCl including 5.0×10^{-3} M $[Fe(CN)_6]^{3-/4-}$ and (D) the corresponding calibration plots between different scan rates versus anodic(Ipa) and cathodic peak current(Ipc).

The effect of scan rate on the current response of the SPE/P-Cys@AuNP sensor was confirmed by a series of CVs analysis of the redox probe (5.0×10^{-3} M $[Fe(CN)_6]^{3-/4-}$ containing 0.1 KCl) at different scan rates of 10, 20, 30, 40, 50, 60, 70, 80, 90, 100, 150, 200 mV/s in the potential range of -0.2V to 0.6V as shown in Fig. 2C. In addition, Fig. 2D depicts a linear relationship between the scan rate and oxidation and reduction peak currents suggesting adsorption is controlled on the surface of the modified electrode.

Furthermore, to explore the relationship between peak current of SPE/P-Cys@AuNP and scan rates was also studied. A linear relationship between the scan rates and peak current values was found with excellent correlation coefficients as shown in Fig. 2D, which suggests an absorption-controlled process due to the mass transfer phenomenon at the interface of solution-electrode[44]. Figure 2C represents the CV of SPE/P-Cys@AuNP modified electrode toward *S.* Typhi detection at different scan rates. Several parameters are measured for the optimization of the proposed sensor. The full procedures are described in supplementary section 3.

3.3 Analytical performance of the biosensor

The electrochemical performance of the modified electrode was determined at a series of concentrations of LT ssDNA using the well-defined DPV methods under the optimized conditions. The SPE/P-Cys@AuNP/CP/BSA was used for electrochemical detections of different concentrations of *S.* Typhi and the obtained voltammograms were recorded. As shown in Fig. 3A, 3B, and 3C, the oxidation peak current at around -0.55 V in DPV increased as the concentration of *S.* Typhi increased from 1×10^{-22} $molL^{-1}$ to 1×10^{-6} $molL^{-1}$. Subsequently, a linear relationship between DPV responses and the different concentrations of *S.* Typhi bacteria was studied.

The increasing oxidation currents between pre-and post-hybridization were considered as the measurement signal. The results confirmed that the oxidation peak current is linearly fitted with the logarithm of the concentration of *S.* Typhi gene target sequence within 1×10^{-22} to 1×10^{-6} molL^{-1} (R^2 = 0.998). The calibration curve exhibits two significant linear segments in the range from 1×10^{-10} to 1×10^{-6} molL^{-1} (R^2 = 0.9918) (Fig. 3B), and 1×10^{-22} to 1×10^{-10} molL^{-1} (R^2 = 0.9921) (Fig. 3C), with a detection limit (S/N = 3) of 6.8×10^{-25} molL^{-1}.

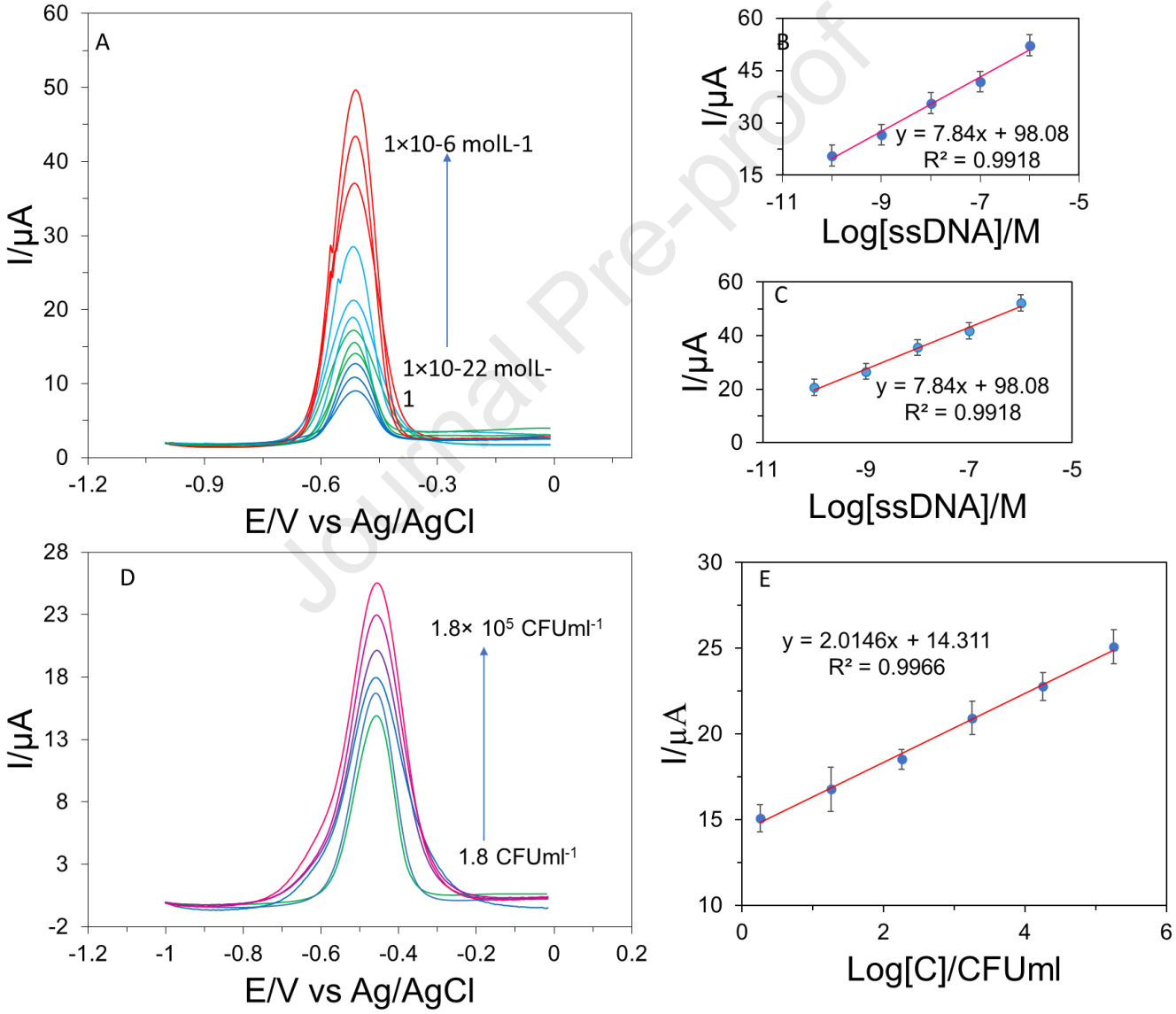

Figure 3: DPV response curve of SPE/P-Cys@AuNP/CP/BSA after hybridization with 1×10^{-22} to 1×10^{-6} molL^{-1} linear target ssDNA in 0.01molL^{-1} phosphate buffer containing 1×10^{-3} molL^{-1} AQMS at a scan rate of 100 mVs^{-1} (A), the corresponding calibration curves of peak currents vs logarithm of linear target ssDNA concentrations (B, C); DPV response to different concentration of *S.* Typhi in real samples (D) DPV for 1×10^{-3} molL^{-1} AQMS and (E) calibration plot of DPV response.

The analytical performance of the DNA biosensor was also validated by DPV analysis of *S.* Typhi isolates which were collected from poultry feces. Detailed procedures for sample collection and identification are discussed in the supplementary information in sections 1-3). Figure 3D illustrates the DPV response of *S.* Typhi ssDNA ranging from 1.8 to 1.8×10^{5} CFUml^{-1} and Fig. 3E shows a linearly fitted logarithm of the concentration of *S.* Typhi in the following range with a LOD of 1 CFUml^{-1}.

Therefore, the designed electrochemical biosensor showed a highly sensitive detection system of *S.* Typhi bacteria with a wide linear response range and a 6.8×10^{-25} molL^{-1} detection limit. High sensitivity is important as the bacterial load in the blood of acute typhoid is low, with an average of < 1 CFU/mL of blood which is maximal during the first week of illness. Meanwhile, owing to the target replacement, the biosensor provided a wide detection range. Moreover, the analytical findings of these electrochemical measurements were compared with DNA biosensors for detection of different *Salmonella spp.* reported in the last few years [28,45–49] as presented in **Table 1.**

Table 1: Performance comparisons of various electrochemical DNA biosensors reported in the literature for detection of *Salmonella* spp.

Electrodes	**Target bacteria**	**Dynamic ranges ($molL^{-1}$)**	**LOD ($molL^{-1}$)**	**LOD (CFU/ml)**	**References**
ITO/GO-CHI	*S. Typhi*	5.0×10^{-8} – 1.0×10^{-14}	1.0×10^{-14}	-	[28]
SPE/MPTS-AuNPs	*S.* Typhi	5.0×10^{-8} – 1.0×10^{-10}	5.0×10^{-11}	-	[45]
GCE/GO/GNPs	*Salmonella*	-	-	3.0	[46]
ITO/GNAs	*S.* Typhi	2.4×10^{-14} – 4.0×10^{-18}	4.0×10^{-18}	-	[47]
Au/Cys/Glu	*S.* Typhi	-	1.91 µg/ml	-	[48]
GCE/Au/NPG	*S.* Typhimurium	-	-	1.0	[49]
SPE/P-Cys@AuNPs	*S.* Typhi	1×10^{-6} – 1×10^{-10} 1×10^{-10} – 1×10^{-22}	6.8×10^{-25}	1.0	The present work

3.4 Selectivity, Stability, reproducibility, and regeneration of the biosensor

To approve the DNA biosensor as a diagnostic tool for detecting *S.* Typhi, an investigation of selectivity to the target of the electrochemical DNA biosensor is very important. For this study, DPV of different base mismatches, different targets ssDNA, and different positive and negative controls (*Salmonella* Typhimurium (*S.* Typhimurium, ATCC 19585), *Escherichia coli* O157*(E. coli)*, *S.* Typhi, *Shigella sonnei (S. sonnei*, ATCC 10908), *Salmonella cotham* (*S. cotham*) were recorded. Figure 4A compares the value of peak intensity of 1×10^{-06} $molL^{-1}$ of different mismatch

ssDNA sequences. As expected, the current response decreased with an increasing number of base mismatches and the current response value of non-complementary targets illustrates a similar current response as the background noise. Figure 4B represents the DPV response of 50ng/µl similar and distant genera of *S.* Typhi. The experiment reveals the current response of *S.* Typhi DNA is the largest whilst the other Salmonella spp. exhibit a much lower current response closer to the current response of the control. Due to some similarities in base sequence between *S.* Typhimurium and *S.* Cotham and *S*. Typhi, a higher current response is shown for these bacterial species than E. coli and *S. sonnei*[50]. So, the result of this study reveals the biosensor can detect *S*. Typhi with relatively high selectivity.

The stability of the DNA biosensor is the most important parameter to validify the practical application in real-time for bacteria detection. To access the stability of the biosensor, a set of GCE/P-Cys@Au/CP/BSA electrodes were stored at 4˚C, and DPV of *S.* Typhi ssDNA sequence was recorded after binding with RP every 7 days over 8 weeks. Figure 4C illustrates how the stability changes with storage which revealed the biosensor remained stable from 0 to 5 weeks with a minimal change in the stability observed up until week 7., However, a dramatic change was found after 8 weeks of storage dropping instability to 90 % which is quite similar to the previously reported biosensors for detecting *S.* Typhi [28,47].

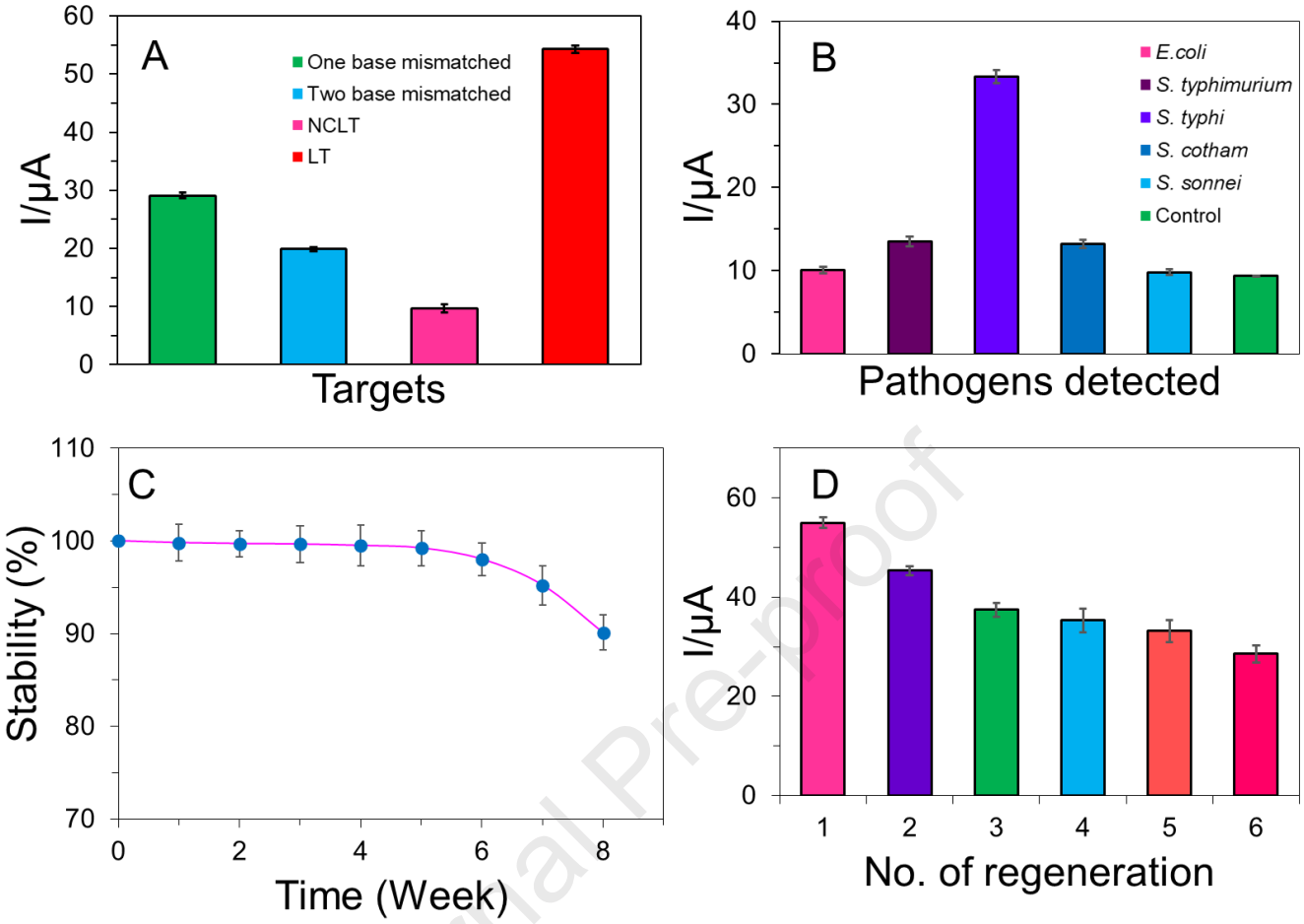

Figure 4: Current response of different target ssDNA (A) and different pathogenic bacteria (B); stability profile of SPE/P-Cys@AuNP/CP/BSA after storage periods (weeks) at 4˚C (C) and regeneration analysis of the DNA biosensor by using 0.1 molL^{-1}NaOH (D).

The reproducibility of the DNA biosensor was evaluated by taking a series of DPV measurements of target sequences of the same concentration by using the modified electrode under certain optimized conditions. The relative standard deviation (RSD) was determined by using five repetitive DPV measurements. The calculated RSD value is 1.08% indicating that the DNA biosensor exhibits better consistency in the detection of *S.* Typhi than the previously reported work [47].

The regeneration of the proposed biosensor was determined by treating the hybridized electrode for 5 min with 0.1 $molL^{-1}$ NaOH to break the hybridized DNA duplex and rebind 1×10^{-6} $molL^{-1}$ LT. Then, DPV measurements of the electrode were recorded in the presence of AQMS in PBS which is shown in Fig. 4D. The current response declined with the number of times of regeneration due to a breaking of the bonding between the crosslinker and CP during NaOH treatment. This biosensor response of 6 to 7 repetitive assembly and disassembly cycles was similar to previously reported work [45,47].

3.5 Application of the electrochemical DNA biosensor in the detection of real samples

To demonstrate the electrochemical DNA biosensor as an effective tool for monitoring *S.* Typhi in food and poultry industries, a recovery test in the spiked sample (blood, poultry faeces, egg, and milk) was conducted in the presence of 2.1×10^{5} $CFUml^{-1}$ containing 1×10^{-3} $molL^{-1}$ AQMS. The electrochemical biosensor exhibited excellent recoveries ranging from 96.54% to 103.47% (**Table S3**) which indicates the impurities of the spiked sample didn't create any significant disturbance in the detection of *S.* Typhi.

4.0 Conclusion

In summary, a novel electrochemical DNA biosensor was fabricated to measure the quantity of *S. Typhi* by using the increased peak current response of a signal indicator AQMS. The SPE was modified by a composite of P-Cys and AuNP which was confirmed by SEM and ATR-FTIR and thereafter immobilized with different detection probes. The feasibility of the DNA biosensor was investigated by CV, EIS, and monitoring the *S. Typhi* concentration-dependent DPV response. To attain the best analytical performance of the biosensor, different parameters were optimized. The biosensor demonstrated a wide range of detection and relatively high selectivity to detect S. Typhi

compared to dissimilar sequences and other bacteria. The recovery test of the DNA biosensor in the spiked sample revealed that the developed biosensor has the potential to be highly suitable for this application and can be illustrated as a model methodology for the determination of other pathogens. Considering the current biosensor's performance shown in selectivity, stability, reusability, reproducibility, and LOD, the use of the proposed strategy to measure *S.* Typhi is most ingenious. Therefore, this designed biosensing platform illustrates the opportunity to bring a revolution in the diagnosis of typhoid and screening of *S.* Typhi from real samples. However, a full intra and inter-laboratory validation of the performance parameters compared to the current state-of-the-art analytical methods with the inclusion of different Salmonella spp. including different serotypes of *S.* Typhi and varying concentrations of other bacterium as blind samples would be the next stage to prove this sensor model truly fit for purpose.

Author declaration

The authors declare that there is no conflict of interest in this work.

Acknowledgment:

The work has been done with the financial support from the Ministry of Information and Communication Technology, Government of Bangladesh (Innovation Fund).

References

[1] S. Campuzano, P. Yáñez-Sedeño, J.M. Pingarrón, Electrochemical affinity biosensors in food safety, Chemosensors. 5 (2017). https://doi.org/10.3390/chemosensors5010008.

[2] J. Chen, R.A. Picard, D. Wang, S.R. Nugen, Lyophilized Engineered Phages for Escherichia coli Detection in Food Matrices, ACS Sensors. 2 (2017) 1573–1577. https://doi.org/10.1021/acssensors.7b00561.

[3] S.P. Ravindranath, L.J. Mauer, C. Deb-roy, J. Irudayaraj, Integrated Mid-Infrared Pathogen Sensor for Food Matrixes, Anal. Biochem. 81 (2009) 2840–2846.

[4] N. Reta, C.P. Saint, A. Michelmore, B. Prieto-Simon, N.H. Voelcker, Nanostructured Electrochemical Biosensors for Label-Free Detection of Water- and Food-Borne Pathogens, ACS Appl. Mater. Interfaces. 10 (2018) 6055–6072. https://doi.org/10.1021/acsami.7b13943.

[5] N. Ansari, R. Yazdian-Robati, M. Shahdordizadeh, Z. Wang, K. Ghazvini, Aptasensors for quantitative detection of Salmonella Typhimurium, Anal. Biochem. 533 (2017) 18–25. https://doi.org/10.1016/j.ab.2017.06.008.

[6] N.F.D. Silva, J.M.C.S. Magalhães, C. Freire, C. Delerue-Matos, Electrochemical biosensors for Salmonella: State of the art and challenges in food safety assessment, Biosens. Bioelectron. 99 (2018) 667–682. https://doi.org/10.1016/j.bios.2017.08.019.

[7] F.J. Bula-Rudas, M.H. Rathore, N.F. Maraqa, Salmonella Infections in Childhood, Adv. Pediatr. 62 (2015) 29–58. https://doi.org/10.1016/j.yapd.2015.04.005.

[8] J. Dong, H. Zhao, M. Xu, Q. Maa, S. Ai, A label-free electrochemical impedance

immunosensor based on AuNPs/PAMAM-MWCNT-Chi nanocomposite modified glassy carbon electrode for detection of Salmonella typhimurium in milk, Food Chem. 141 (2013) 1980–1986. https://doi.org/10.1016/j.foodchem.2013.04.098.

[9] G.J. Yang, J.L. Huang, W.J. Meng, M. Shen, X.A. Jiao, A reusable capacitive immunosensor for detection of Salmonella spp. based on grafted ethylene diamine and self-assembled gold nanoparticle monolayers, Anal. Chim. Acta. 647 (2009) 159–166. https://doi.org/10.1016/j.aca.2009.06.008.

[10] X.L. Zhang, V.T. Jeza, Q. Pan, Salmonella typhi: From a human pathogen to a vaccine vector, Cell. Mol. Immunol. 5 (2008) 91–97. https://doi.org/10.1038/cmi.2008.11.

[11] R. Jarquin, I. Hanning, S. Ahn, S.C. Ricke, Development of rapid detection and genetic characterization of Salmonella in poultry breeder feeds, Sensors. 9 (2009) 5308–5323. https://doi.org/10.3390/s90705308.

[12] M.E. Ohanu, A.U. Mbah, P.O. Okonkwo, F.S. Nwagbo, Interference by malaria in the diagnosis of typhoid using Widal test alone., West Afr. J. Med. 22 (2003) 250–252. https://doi.org/10.4314/wajm.v22i3.27961.

[13] H. Xu, H.Y. Lee, J. Ahn, Growth and virulence properties of biofilm-forming Salmonella enterica serovar Typhimurium under different acidic conditions, Appl. Environ. Microbiol. 76 (2010) 7910–7917. https://doi.org/10.1128/AEM.01508-10.

[14] P. Pashazadeh, A. Mokhtarzadeh, M. Hasanzadeh, M. Hejazi, M. Hashemi, M. de la Guardia, Nano-materials for use in sensing of salmonella infections: Recent advances, Biosens. Bioelectron. 87 (2017) 1050–1064. https://doi.org/10.1016/j.bios.2016.08.012.

[15] A. Bétard, R.A. Fischer, Metal-organic framework thin films: From fundamentals to applications, Chem. Rev. 112 (2012) 1055–1083. https://doi.org/10.1021/cr200167v.

[16] W. Wang, X. Fan, S. Xu, J.J. Davis, X. Luo, Low fouling label-free DNA sensor based on polyethylene glycols decorated with gold nanoparticles for the detection of breast cancer biomarkers, Biosens. Bioelectron. 71 (2015) 51–56. https://doi.org/10.1016/j.bios.2015.04.018.

[17] W. Xu, T. Jin, Y. Dai, C.C. Liu, Surpassing the detection limit and accuracy of the electrochemical DNA sensor through the application of CRISPR Cas systems, Biosens. Bioelectron. 155 (2020) 112100. https://doi.org/10.1016/j.bios.2020.112100.

[18] R. Chauhan, J. Singh, T. Sachdev, T. Basu, B.D. Malhotra, Recent advances in mycotoxins detection, Biosens. Bioelectron. 81 (2016) 532–545. https://doi.org/10.1016/j.bios.2016.03.004.

[19] H. Liu, R. Xiong, P. Zhong, G. Li, J. Liu, J. Wu, Y. Liu, Q. He, Nanohybrids of shuttle-like α-Fe2O3nanoparticles and nitrogen-doped graphene for simultaneous voltammetric detection of dopamine and uric acid, New J. Chem. 44 (2020) 20797–20805. https://doi.org/10.1039/d0nj04629a.

[20] A.R. Unnithan, A.R.K. Sasikala, P. Murugesan, M. Gurusamy, D. Wu, C.H. Park, C.S. Kim, Electrospun polyurethane-dextran nanofiber mats loaded with Estradiol for post-menopausal wound dressing, Int. J. Biol. Macromol. 77 (2015) 1–8. https://doi.org/10.1016/j.ijbiomac.2015.02.044.

[21] Q. Li, J.T. Wu, Y. Liu, X.M. Qi, H.G. Jin, C. Yang, J. Liu, G.L. Li, Q.G. He, Recent advances in black phosphorus-based electrochemical sensors: A review, Anal. Chim.

Acta. 1170 (2021) 338480. https://doi.org/10.1016/j.aca.2021.338480.

[22] Q. Li, Y. Xia, X. Wan, S. Yang, Z. Cai, Y. Ye, G. Li, Morphology-dependent MnO2/nitrogen-doped graphene nanocomposites for simultaneous detection of trace dopamine and uric acid, Mater. Sci. Eng. C. 109 (2020) 110615. https://doi.org/10.1016/j.msec.2019.110615.

[23] M.H. Mat Zaid, J. Abdullah, N.A. Yusof, Y. Sulaiman, H. Wasoh, M.F. Md Noh, R. Issa, PNA biosensor based on reduced graphene oxide/water soluble quantum dots for the detection of Mycobacterium tuberculosis, Sensors Actuators, B Chem. 241 (2017) 1024–1034. https://doi.org/10.1016/j.snb.2016.10.045.

[24] M.H.M. Zaid, J. Abdullah, N. Rozi, A.A.M. Rozlan, S.A. Hanifah, A sensitive impedimetric aptasensor based on carbon nanodots modified electrode for detection of 17ß-estradiol, Nanomaterials. 10 (2020) 1–14. https://doi.org/10.3390/nano10071346.

[25] J. Zhang, Y. Li, S. Duan, F. He, Highly electrically conductive two-dimensional Ti3C2 Mxenes-based 16S rDNA electrochemical sensor for detecting Mycobacterium tuberculosis, Anal. Chim. Acta. 1123 (2020) 9–17. https://doi.org/10.1016/j.aca.2020.05.013.

[26] M. Rahman, L.Y. Heng, D. Futra, T.L. Ling, Ultrasensitive Biosensor for the Detection of Vibrio cholerae DNA with Polystyrene-co-acrylic Acid Composite Nanospheres, Nanoscale Res. Lett. 12 (2017). https://doi.org/10.1186/s11671-017-2236-0.

[27] B. Hatamluyi, Z. Es'haghi, Quantitative Biodetection of Anticancer Drug Rituxan with DNA Biosensor Modified PAMAM Dendrimer/Reduced Graphene Oxide Nanocomposite, Electroanalysis. 30 (2018) 1651–1660.

https://doi.org/10.1002/elan.201800014.

[28] A. Singh, G. Sinsinbar, M. Choudhary, V. Kumar, R. Pasricha, H.N. Verma, S.P. Singh, K. Arora, Graphene oxide-chitosan nanocomposite based electrochemical DNA biosensor for detection of typhoid, Sensors Actuators, B Chem. 185 (2013) 675–684. https://doi.org/10.1016/j.snb.2013.05.014.

[29] V. Gaudin, Advances in biosensor development for the screening of antibiotic residues in food products of animal origin – A comprehensive review, Biosens. Bioelectron. 90 (2017) 363–377. https://doi.org/10.1016/j.bios.2016.12.005.

[30] J.I.A. Rashid, N.A. Yusof, The strategies of DNA immobilization and hybridization detection mechanism in the construction of electrochemical DNA sensor: A review, Sens. Bio-Sensing Res. 16 (2017) 19–31. https://doi.org/10.1016/j.sbsr.2017.09.001.

[31] M.Z.H. Khan, M.S. Ahommed, M. Daizy, Detection of xanthine in food samples with an electrochemical biosensor based on PEDOT:PSS and functionalized gold nanoparticles, RSC Adv. 10 (2020) 36147–36154. https://doi.org/10.1039/d0ra06806c.

[32] F. Zheng, P. Wang, Q. Du, Y. Chen, N. Liu, Simultaneous and ultrasensitive detection of foodborne bacteria by gold nanoparticles-amplified microcantilever array biosensor, Front. Chem. 7 (2019). https://doi.org/10.3389/fchem.2019.00232.

[33] L.C. Umuhumuza, X. Sun, Rapid detection of pork meat freshness by using L-cysteine-modified gold electrode, Eur. Food Res. Technol. 232 (2011) 425–431. https://doi.org/10.1007/s00217-010-1405-5.

[34] D.S. Campos-Ferreira, G.A. Nascimento, E.V.M. Souza, M.A. Souto-Maior, M.S. Arruda,

D.M.L. Zanforlin, M.H.F. Ekert, D. Bruneska, J.L. Lima-Filho, Electrochemical DNA biosensor for human papillomavirus 16 detection in real samples, Anal. Chim. Acta. 804 (2013) 258–263. https://doi.org/10.1016/j.aca.2013.10.038.

[35] A.C.M. Ferreon, C.R. Moran, Y. Gambin, A.A. Deniz, Single-Molecule Fluorescence Studies of Intrinsically Disordered Proteins, 1st ed., Elsevier Inc., 2010. https://doi.org/10.1016/S0076-6879(10)72010-3.

[36] M.Z.H. Khan, M. Daizy, C. Tarafder, X. Liu, Au-PDA@SiO2 core-shell nanospheres decorated rGO modified electrode for electrochemical sensing of cefotaxime, Sci. Rep. 9 (2019). https://doi.org/10.1038/s41598-019-55517-9.

[37] M.R. Ali, M.S. Bacchu, M.R. Al-Mamun, M.M. Rahman, M.S. Ahommed, M.A.S. Aly, M.Z.H. Khan, Sensitive MWCNT/P-Cys@MIP sensor for selective electrochemical detection of ceftizoxime, J. Mater. Sci. 56 (2021) 12803–12813. https://doi.org/10.1007/s10853-021-06115-6.

[38] O.C. Ozoemena, T. Maphumulo, J.L. Shai, K.I. Ozoemena, Electrospun Carbon Nanofibers as an Electrochemical Immunosensing Platform for Vibrio cholerae Toxin: Aging Effect of the Redox Probe, ACS Omega. 5 (2020) 5762–5771. https://doi.org/10.1021/acsomega.9b03820.

[39] S. Yang, P. Liu, Y. Wang, Z. Guo, reduced graphene oxide for detection of lead ions †, (2020) 18526–18532. https://doi.org/10.1039/d0ra03149f.

[40] M. Ashjari, S. Dehfuly, D. Fatehi, R. Shabani, M. Koruji, Efficient functionalization of gold nanoparticles using cysteine conjugated protoporphyrin IX for singlet oxygen production in vitro, RSC Adv. 5 (2015) 104621–104628.

https://doi.org/10.1039/c5ra15862a.

[41] S.R. Ankireddy, J. Kim, Selective detection of dopamine in the presence of ascorbic acid via fluorescence quenching of inp/zns quantum dots, Int. J. Nanomedicine. 10 (2015) 113–119. https://doi.org/10.2147/IJN.S88388.

[42] M. Rahman, D. Cui, S. Zhou, A. Zhang, D. Chen, A graphene oxide coated gold nanostar based sensing platform for ultrasensitive electrochemical detection of circulating tumor DNA, Anal. Methods. 12 (2020) 440–447. https://doi.org/10.1039/c9ay01620a.

[43] R. Cai, Z. Zhang, H. Chen, Y. Tian, N. Zhou, A versatile signal-on electrochemical biosensor for Staphylococcus aureus based on triple-helix molecular switch, Sensors Actuators, B Chem. 326 (2021). https://doi.org/10.1016/j.snb.2020.128842.

[44] M.Z.H. Khan, X. Liu, Y. Tang, J. Zhu, W. Hu, X. Liu, A glassy carbon electrode modified with a composite consisting of gold nanoparticle, reduced graphene oxide and poly(L-arginine) for simultaneous voltammetric determination of dopamine, serotonin and L-tryptophan, Microchim. Acta. 185 (2018) 3–12. https://doi.org/10.1007/s00604-018-2979-z.

[45] R. Das, M.K. Sharma, V.K. Rao, B.K. Bhattacharya, I. Garg, V. Venkatesh, S. Upadhyay, An electrochemical genosensor for Salmonella typhi on gold nanoparticles-mercaptosilane modified screen printed electrode, J. Biotechnol. 188 (2014) 9–16. https://doi.org/10.1016/j.jbiotec.2014.08.002.

[46] X. Ma, Y. Jiang, F. Jia, Y. Yu, J. Chen, Z. Wang, An aptamer-based electrochemical biosensor for the detection of Salmonella, J. Microbiol. Methods. 98 (2014) 94–98. https://doi.org/10.1016/j.mimet.2014.01.003.

[47] A. Singh, M. Choudhary, M.P. Singh, H.N. Verma, S.P. Singh, K. Arora, DNA Functionalized Direct Electro-deposited Gold nanoaggregates for Efficient Detection of Salmonella typhi, Bioelectrochemistry. 105 (2015) 7–15. https://doi.org/10.1016/j.bioelechem.2015.03.005.

[48] W.N. Suryapratiwi, V.I. Paat, S. Gaffar, Y.W. Hartati, DNA biosensor for detection of Salmonella typhi from blood sample of typhoid fever patient using gold electrode modified by self-assembled monolayers of thiols, in: AIP Conf. Proc., American Institute of Physics Inc., 2017. https://doi.org/10.1063/1.4983937.

[49] S. Ranjbar, S. Shahrokhian, F. Nurmohammadi, Nanoporous gold as a suitable substrate for preparation of a new sensitive electrochemical aptasensor for detection of Salmonella typhimurium, Sensors Actuators, B Chem. 255 (2018) 1536–1544. https://doi.org/10.1016/j.snb.2017.08.160.

[50] M.R. Ali, M.S. Bacchu, M.A.A. Setu, S. Akter, M.N. Hasan, F.T. Chowdhury, M.M. Rahman, M.S. Ahommed, M.Z.H. Khan, Development of an advanced DNA biosensor for pathogenic Vibrio cholerae detection in real sample, Biosens. Bioelectron. 188 (2021) 113338. https://doi.org/10.1016/j.bios.2021.113338.

Highlights

- The newest electrochemical DNA biosensor for *Salmonella* Typhi detection was presented.
- The sensor fabricated by immobilizing an amine labelled *S.* Typhi specific single-strand capture probe
- The biosensor shows a detection range of 1×10^{-6} to 1×10^{-22} $molL^{-1}$ with a LOD of 6.8×10^{-25} $molL^{-1}$
- The ability to reuse the biosensor more than 6 to 7 times was observed
- The fabricated biosensor found useful for selective identification of *S.* Typhi in real samples

Declaration of Interest Statement by authors

The authors declare that there is no conflict of interest.